European Surgical Research
Eur Surg Res 2018;59:128–142
DOI: 10.1159/000490663
Received: August 24, 2017
Accepted: June 6, 2018
Published online: August 8, 2018

Original Paper

The MRI Sepsis Score: An Innovative Tool for the Evaluation of Septic Peritonitis in Mice Using 7-Tesla Small Animal MRI

Stephan Diedrich[a] Julia van der Linde[a] Michael Nielson[a] Pia Menges[a] Jens-Peter Kühn[b, c] Andre Käding[a] Dung Ngyuen Trung[a] Claus-Dieter Heidecke[a] Lars Ivo Partecke[a] Wolfram Kessler[a]

[a]Department of General, Visceral, Thoracic and Vascular Surgery, Universitätsmedizin Greifswald, Greifswald, Germany; [b]Department of Diagnostic Radiology and Neuroradiology, Universitätsmedizin Greifswald, Greifswald, Germany; [c]Institute of Radiology, University Hospital Dresden, Carl-Gustav-Carus University Dresden, Dresden, Germany

Keywords
Sepsis · CASP model · Small animal MRI · Sepsis score · Morphologic changes

Abstract
Background: Magnetic resonance imaging (MRI) techniques are rarely used in the context of abdominal sepsis and in sepsis research. This study investigates the impact of MRI for monitoring septic peritonitis in an animal model (colon ascendens stent-induced peritonitis, CASP). The CASP model closely mimics that of human disease and is highly standardized. The most frequently employed readout parameter in mouse CASP studies is prolonged or decreased rate of survival. Monitoring the progression of peritonitis via MRI could provide a helpful tool in the evaluation of severity. The use of alternative readout systems could very well reduce the number of research animals. Perspectively, clinical improvement after certain treatment could be classified. ***Methods:*** This study describes for the first time MRI findings following the induction of septic peritonitis in mice using the CASP model. Two sublethal groups of mice with septic peritonitis were investigated. Each had received one of two differing stent diameters in order to control the leakage of feces into the abdominal cavity. Each mouse served as its own control. Imaging and analyses were performed blinded. Gut diameters, stomach volume, abdominal organ wall diameters, and volume of the adrenal glands were measured. Serum corticosterone levels were detected using ELISA. Serum IL-6, TNF-α, IL-1β, and IL-10

Lars Ivo Partecke and Wolfram Kessler contributed to this work and share last authorship.

Dr. med. Stephan Diedrich
Department of General, Visceral, Thoracic and Vascular Surgery
Universitätsmedizin Greifswald, Ferdinand-Sauerbruch-Strasse
DE–17475 Greifswald (Germany)
E-Mail diedrich@uni-greifswald.de

Eur Surg Res 2018;59:126–142
DOI: 10.1159/000490663

levels were screened by cytometric bead array. Statistical analysis was performed using the Mann-Whitney U test for nonparametric probes and the Kruskal-Wallis and *t* tests. ***Results:*** Using a 7-tesla MRI scanner 24 and 48 h after induction of septic peritonitis, interenteric fluid, organ swelling of spleen and adrenal glands, as well as dilatation of the stomach were compared to nonseptic conditions. Swelling of adrenal glands resulted in an increased serum corticosterone level. In addition, the wall of the intestine bowel was thickened. Based upon these findings, an MRI score (MRI sepsis score, MSS) for abdominal sepsis in mice was established. Reduced stent sizes led to reduced severity of the abdominal sepsis, which could be reproduced in the MSS, which is described here for the first time. ***Conclusions:*** Intraabdominal variations during septic peritonitis are detectable by MRI techniques. MRI methods should become a more important tool for the evaluation of abdominal peritonitis. MSS could provide an interesting tool for the evaluation of therapeutic strategies.

Introduction

Severe sepsis and septic shock are major clinical syndromes associated with high morbidity, mortality, and costs [1]. Sepsis is the leading cause of death in critically ill patients [2] and its incidence remains increasing [3]. Early identification of abdominal sepsis is difficult, requiring sophisticated experience of the physician. In surgical intensive care units radiological techniques such as computed tomography (CT) and magnetic resonance imaging (MRI) are essential in detecting septic focus. Repetitive CT scans, however, lead to highly accumulative doses of radiation, and iodine contrast agents increase the risk for nephrotoxicity. Subsequently, the kidney is stressed in a situation where additional organ failure could determine the clinical course of sepsis [4].

The colon ascendens stent-induced peritonitis (CASP) model correlates with the clinical course of a polymicrobial sepsis induced by the perforation of gastrointestinal organs or anastomosis leakage [5]. A previous study describing high-definition imaging of abdominal organs in a murine pancreatic cancer model using 7-tesla MRI evaluated its clinical relevance and applicability [6].

The aim of this study was to evaluate the impact of small animal MRI technology for monitoring inflammatory response in the abdomen. To the best of our knowledge, there are no published data showing the course of a septic peritonitis using MRI. This investigation could show the progression of peritonitis for the first time using the murine CASP method. Two different stent diameters were applied based upon that the well-known survival kinetics for the 18- and 16-G CASP model [7] and early morphologic changes were subsequently visualized by MRI. To establish MRI as a useful tool for monitoring abdominal sepsis, typical clinical signs of peritonitis were detected in the well-established CASP model. The overall aim of the study was to establish a reliable score, which could describe the course of septic peritonitis over time. The repetitive visualization of the status quo during the course of abdominal sepsis by MRI could become a useful tool in the diagnosis and treatment of sepsis.

Materials and Methods

Mice

A total of 20 female C57BL/6 mice (8–10 weeks old) were used in all of the experiments. The mice were purchased from Charles River® (Sulzfeld, Germany). Prior to experimental intervention the animals were housed for at least 1 week in our animal facility to recover from transportation. Experimental procedures were performed according to German animal safety regulations. Before starting experiments all animal

studies were approved by the ethics committee for animal care of Mecklenburg-Vorpommern, Germany (Approval code: LALLF M-V/TSD/7221.3-2.4.1-001/08 and LALLF M-V/TSD/7221.3-1.1-039/09).

CASP Surgery

The surgical CASP procedure was performed as previously described in detail [7–9]. The study mice were divided into two groups (10 mice in the 16-G CASP group and 10 mice in the 18-G CASP group). Briefly, the abdominal wall was disinfected and subsequently opened through a 1.5-cm midline incision. After exposure of the ascending colon, the previously prepared 16- or 18-G venous indwelling catheter (Becton-Dickinson, Heidelberg, Germany) was inserted through the antimesenteric wall into the lumen of the ascending colon and fixed by sutures (7-0 Ethilon thread; Ethicon, Norderstedt, Germany). Consecutively, the inner needle of the catheter was removed and the remaining stent was cut at the prepared site. To ensure proper intraluminal positioning of the stent, stool was milked out of the cecum into the ascending colon via the stent, until a droplet of stool appeared. Fluid resuscitation was performed by flushing 0.3 mL of sterile saline solution into the peritoneal cavity of the animals before closure of the abdominal walls (two layers, muscle and skin; 4-0 Ethilon thread). In a separate group, 4 mice underwent abdominal wall opening and closure only (sham group).

MRI Imaging and Image Analyses

For all MRI studies anesthesia was carried out using isoflurane (1–1.5%). The depth of anesthesia was monitored by the breathing rate (about 40 breaths/min). MRI sequences were triggered by the breathing rate. To reduce the influence of bowel motility in all MRI examinations, mice were always kept *nil per os* for at least 4 h prior to the initiation of MRI scans. All mice were maintained in a supine position during the MRI scans. Each mouse served as its own control. Scans were performed prior to surgical intervention (CASP procedure) (timepoint 0) and at 24 and at 48 h after CASP. Mice who underwent laparotomy only (sham) were scanned at 24 h postoperatively.

Mice were scanned in a high-field 7-tesla MRI scanner for small animals (ClinScan, 7-tesla, 290 mtesla/m gradient strength (Bruker, Ettlingen, Germany) as previously described [6]. MRI analyses were performed in a whole mouse body coil (Bruker) using a T2 TSE (turbo spin echo) sequence. Assessment of diameter and volume were carried out via high-resolution conventional T2-weighted images in transverse and coronal orientation (transverse plane: TR [repetition time]: ca. 1,200 ms, TE (echo time): 41.0 ms, FA (flip angle): 180°, FoV (field of view): 42 mm × 42 mm, matrix: 240 × 320, 24 slices of 0.7 mm per slice, acquisition time: ca. 15 min; coronal plane: TR: ca. 1,250 ms, TE: 41.0 ms, FA: 180°, FoV: 40 mm × 40 mm, matrix: 240 × 320, 24 slices of 0.7 mm per slice, acquisition time: ca. 10 min).

Generated images were analyzed blinded using MIPAV (medical imaging processing and visualization; National Institutes of Health, Bethesda, MD, USA) and Image J (Image Processing and Analysis in Java, National Institutes of Health). By defining so-called regions of interest on each slice, the software was able to calculate the volumes and diameters. This was subsequently achieved with a standardized algorithm using all image inherent information including thickness of slices, resolution, as well as size of regions of interest.

The diameter of both adrenal glands was measured in each animal. In addition, the volumes of the stomach and the spleen were calculated using segmentation of MR images. Furthermore, the diameters of the small intestine and the colon were measured in at least 10 subsequent transverse slices per measurement, resulting overall in 300 measuring points in wall thickness and 150 measuring points in lumina in each animal.

MRI Sepsis Score

Scoring of spleen volume, adrenal gland size, stomach volume, characteristics of free fluid, and small intestinal changes facilitated classification of the severity of abdominal morphologic changes with an MRI sepsis score (MSS) system.

Measurement of Cytokines

Blood was collected initially from the untreated mice at timepoint 0, and again at 24 and 48 h after the surgical procedure (16-G CASP). Blood was collected via retroorbital puncture into heparinized syringes (sodium heparin; Ratiopharm, Ulm, Germany) and the cells were subsequently removed by centrifugation (7,000 *g*, 10 min, 4 °C). Tumor necrosis factor alpha (TNF-α), interleukin (IL)-6 and IL-10 concentrations in the plasma were determined using the Cytometric Bead Array-Mouse Inflammation Kit (BD Biosciences Pharmingen, San Diego, CA, USA) as well as a commercially available IL-1β ELISA (BD Biosciences) according to the manufacturer's instructions. All mice were sacrificed 48 h after CASP surgery.

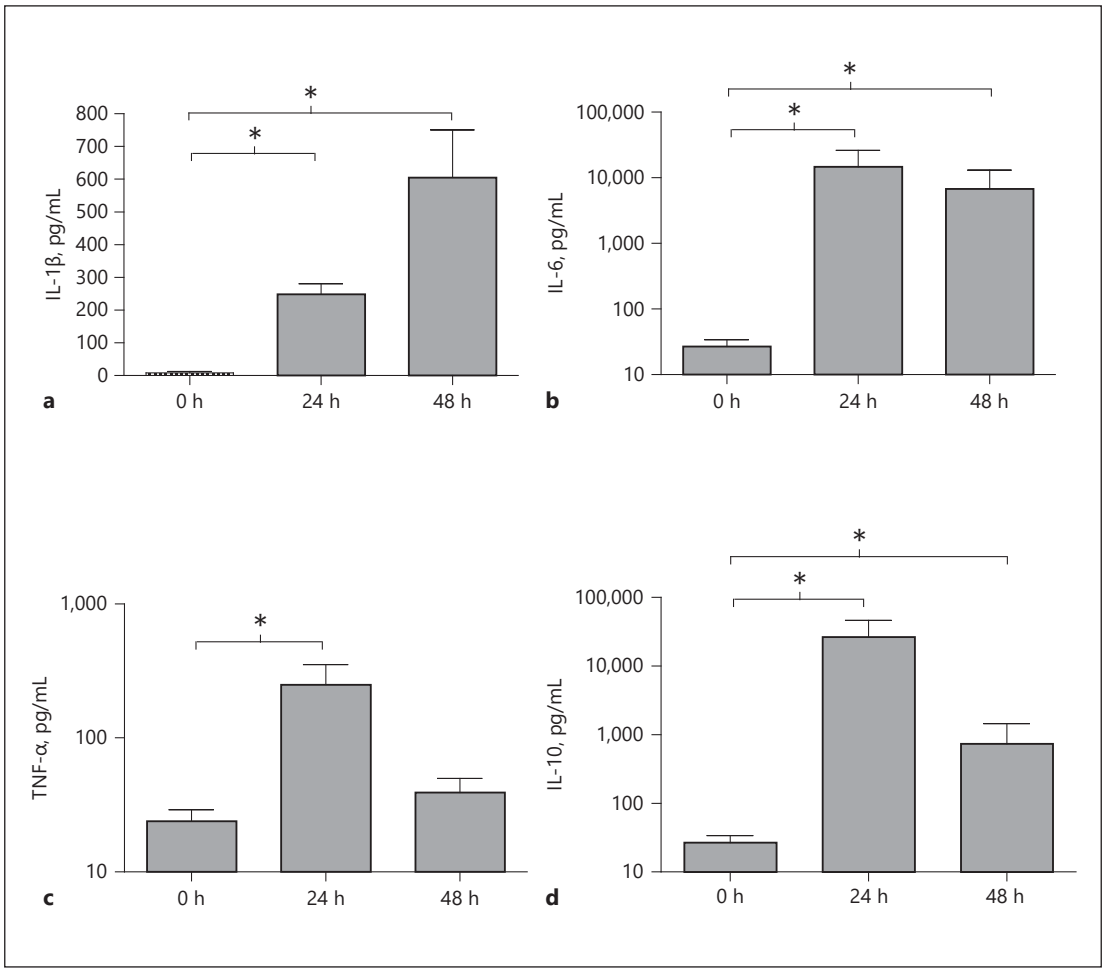

Fig. 1. Serum cytokines IL-1 (**a**), IL-6 (**b**), TNF-α (**c**), and IL-10 (**d**) at 0, 24, and 48 h after CASP. Error bars indicate standard errors of the means (n = 6–10/group). * $p < 0.05$.

Measurement of Corticosterone Levels

Plasma corticosterone levels were quantified by ELISA according to the instructions of the supplier (OCTEIA Corticosterone EIA; IDS, Boldon, UK) with a detection limit of 0.23 ng/ml and interassay variation of 5.6–9.6% for corticosterone. Blood collections through retroorbital puncture were performed before CASP and 12, 24, and 48 h after CASP.

Histology

Three representative mice were sacrificed from the 16-G CASP group as well as from the untreated group (timepoint 0) and examined by necropsy. Paraffin-embedded specimens were consistently cut into 3-µm sections utilizing a Microtom (Leica, Wetzlar, Germany). Histology was performed with H&E staining. The sections were examined using a Leica light microscope.

Statistical Methods

Statistical analysis was performed using GraphPad Prism 5 for Windows software (GraphPad Software, San Diego, CA, USA). ELISA results were analyzed by the two-tailed Mann-Whitney U test for nonparametric probes. Cytokine levels were analyzed using the Kruskal-Wallis test with Dunn's post hoc test for multiple comparisons of nonparametric probes. MRI data and histology data were analyzed by t test. A significance level of 0.05 was determined for all calculations.

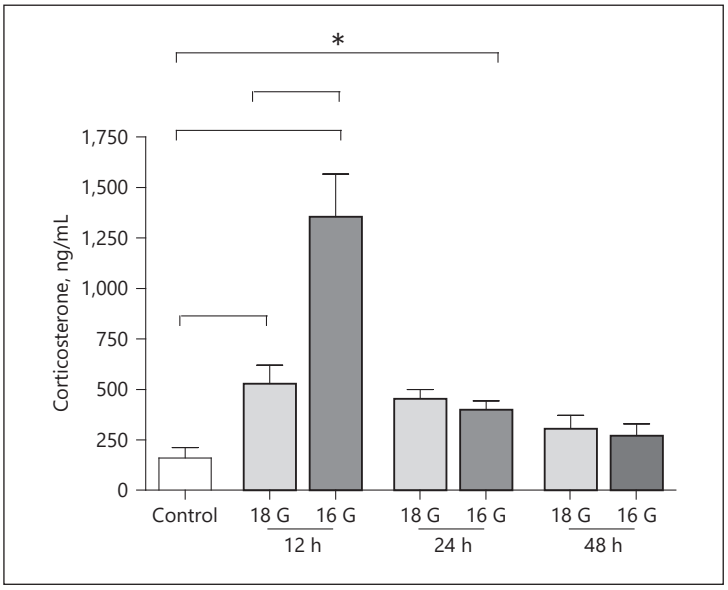

Fig. 2 Serum corticosterone in control and at 12, 24, and 48 h after 18- and 16-G CASP. Error bars indicate standard errors of the means (n = 6–10/group). * p < 0.05.

Results

Classical Proof of Sepsis after CASP

Indications of sepsis in the animals were documented by cytokine levels after 16-G CASP to prove the septic status of the mice. As expected, the CASP procedure resulted in a strong induction of serum cytokines (Fig. 1).

The IL-1β base rate was 7.8 pg/mL (range 1–25 pg/mL, mean 7.8 ± 4.7 pg/mL). Levels increased 24 h after CASP to 238.5 pg/ml (range 174.6–367.4 pg/mL, mean 238.5 ± 36.6 pg/mL) and, 48 h later, to 606 pg/mL (range 284.4–1,037.5 pg/mL, mean 606 ± 114.24 pg/mL).

TNF-α levels in healthy animals were detected at 23.7 pg/mL (range10.2–42.5 pg/mL, mean 23.7 ± 5.5 pg/mL). At 24 h after CASP, a strong increase to 248.31 pg/mL (range 47–651.5 pg/mL, mean 248.31 ± 94.5 pg/mL) was detected. As an early marker it decreased after 48 h to 39.4 pg/mL (range 15.7–84.7 pg/mL, mean 39.4 ± 10.2 pg/mL).

Prior to CASP, IL-10 levels were measured at 26.91 pg/mL (range 11.2–50.7 pg/mL, mean 26.91 ± 6.9 pg/mL). A massive elevation could be detected 24 h following CASP with 25,704 pg/mL (range 10,654–102,028 pg/mL, mean 25,704 ± 15,034 pg/mL) and 741.31 pg/mL (range 448.7–4,265.6 pg/mL, mean 741.31 ± 607.7 pg/mL) after 48 h.

Similar results were detected for IL-6 levels where the base rate was 26.9 pg/mL (range 11.2–50.7 pg/mL, mean 26.9 ± 5.5 pg/mL). CASP animals showed results of 14,125 pg/mL (range 148–29,359.8 pg/mL, mean 14,125 ± 8,262 pg/mL) at 24 h and 760.8 pg/mL (range 134.7–9,265, mean 760.8 ± 4,459.2 pg/mL) after CASP.

Serum Corticosterone Shows an Initial Peek after CASP Induction

Corticosterone levels increased significantly 12 h after CASP (16 G). At 24 and 48 h after CASP levels returned to control level. Measured levels in control mice (timepoint 0) stood at 159.4 ng/ml (range 90.9–370.7 ng/mL, mean 159.4 ± 119 ng/mL). After 12 h an average value of 1,355.3 ng/mL was measured (range 515–1,608.5 ng/mL, mean 1,355.3 ± 471.9 ng/mL). At 24 h after CASP induction the corticosterone level was 401 ng/mL (range 331.1–556.7 ng/mL, mean 401 ± 93.1 ng/mL). At 48 h after performing CASP, corticosterone levels were measured at 270.2 ng/mL (range 126.3–403.2 ng/mL, mean 270.2 ± 131.7 ng/mL). Values at 24 and 48 h differed significantly from those at 12 h; however, no differences were observed

Eur Surg Res 2018;59:126–142
DOI: 10.1159/000490663

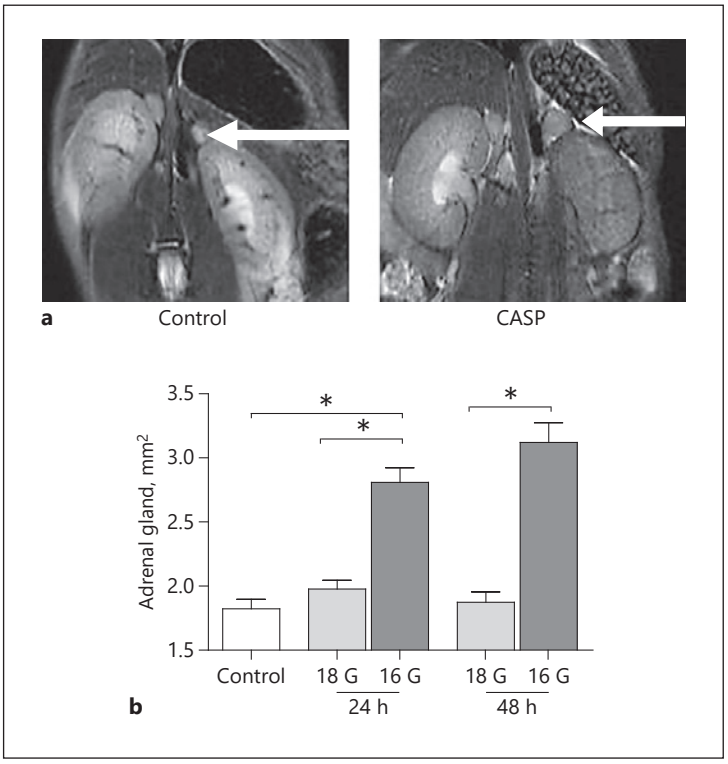

Fig. 3. a Left adrenal gland (white arrows) in control and CASP (coronal sectional image). **b** Adrenal gland size in control and 24 and 48 h after 18- and 16-G CASP. Error bars indicate standard errors of the means (n = 6–10/group). * $p < 0.05$.

in comparison to control mice (timepoint 0). No differences in corticosterone levels were seen with 18-G CASP when compared to 16-G CASP (data not shown) (Fig. 2).

MRI Results in Septic Mice

Laparotomy Only (Sham) Has No Effects on MRI Readout Parameters

In the laparotomy-only group (n = 4) no significant effects on adrenal gland size, spleen volume, bowel diameter, intestinal wall thickness, and free fluid after 24 h could be observed compared to mice at timepoint 0 (see online suppl. data; for all online suppl. material, see www.karger.com/doi/10.1159/000490663).

The Volume of Adrenal Glands as a Marker of Sepsis Severity

The size of adrenal glands increased significantly ($p < 0.05$) following 16-G CASP. CASP surgery using an 18-G stent (18-G CASP) had no effect on gland sizes. In control mice the area of adrenal glands was measured at 1.8 mm^2 (range 1.4–2.0 mm^2, mean 1.8 ± 0.2 mm^2). At 24 h after 16-G CASP, gland size increased to 2.8 mm^2 (range 2.2–3.2 mm^2, mean 2.8 ± 0.4 mm^2, $p < 0.05$). At 48 h after sepsis induction, measured sizes were 3.1 mm^2 (range 2.5–3.9 mm^2, mean 3.1 ± 0.5 mm^2, $p < 0.05$). With the smaller18-G CASP, adrenal gland size remained unchanged at 24 h as well as at 48 h after the operation: 2.0 mm^2 (range 1.7–2.4 mm^2, mean 2.0 ± 0.2 mm^2) and 1.9 mm^2 (range 1.5–2.1mm^2, mean 1.9 ± 0.2 mm^2) (Fig. 3).

Increased Spleen Volume under Septic Conditions

Spleen size was significantly increased after 16-G CASP in comparison to the control group ($p < 0.05$). Usage of a smaller stent did not result in increased spleen volume. The splenic volume of untreated animals was measured at 82 mm^3 (range 68–92 mm^3, mean 82 ± 9 mm^3). At 24 h after 16-G CASP, the volume had increased to 120 mm^3 (range 93–146 mm^3,

Eur Surg Res 2018;59:126–142
DOI: 10.1159/000490663

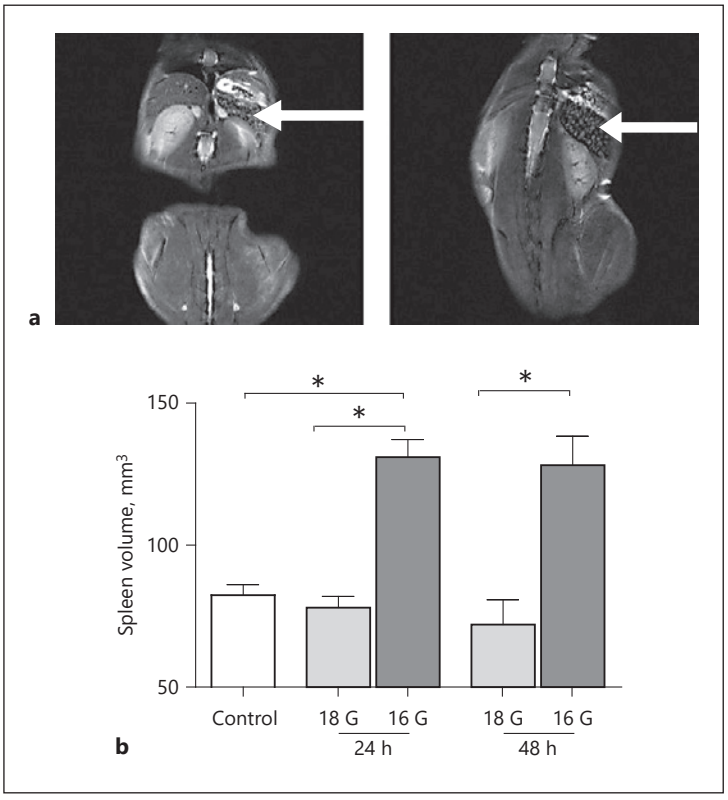

Fig. 4. a Spleen (white arrows) in control and CASP (coronal sectional image). **b** Spleen volume in control and 24 and 48 h after 18- and 16-G CASP. Error bars indicate standard errors of the means (n = 6–10/group). * $p < 0.05$.

mean 120 ± 21 mm^3, $p < 0.05$) and after 48 h to 120 mm^3 (range 96–167 mm^3, mean 120 ± 26 mm^3, $p < 0.05$). With the smaller stent size (18 G) the volume of the spleen after 24 h was 72 mm^3 (range 50–92 mm^3, mean 72 ± 21 mm^3). After 48 h the measured volume was unchanged at 72 mm^3 (range 44–93mm^3, mean 72 ± 17 mm^3) (Fig. 4).

Signs for Intestinal Paralysis under Septic Conditions

Indications of intestinal paralysis could be observed within both groups (18 and 16 G) after CASP (Fig. 5a–f). Measurements of the colon lumen revealed increased diameters in CASP mice (Fig. 5a, b). Animals without peritonitis had an average colon lumen of 3.01 ± 0.72 mm (range 1.49–5.59 mm). 18-G CASP stent insertion resulted in lumen diameters after 24 and 48 h of 3.31 ± 0.95 mm (range 1.6–6.0 mm) and 3.47 ± 0.70 mm (range 1.61–5.95 mm), respectfully ($p < 0.05$). The larger stent diameter (16-G CASP) caused a substantial increase in colon lumina. Values increased to 3.63 ± 0.93 mm (range 1.32–5.81 mm) after 24 h and to 3.71 ± 1.01 mm (range 1.67–5.65 mm) 48 h after the CASP procedure ($p < 0.05$).

In addition, the small intestine showed typical signs of paralysis (Fig. 5c, d). Whereas the small intestines of mice without septic peritonitis revealed an average diameter of 2.24 mm (range 0.6–5.74 mm, mean 2.24 ± 0.75 mm), 24 h after 16-G CASP an average diameter of 2.95 mm (range 1.13–5.25 mm, mean 2.96 ± 0.75 mm, $p < 0.05$) was determined. At 48 h the diameter was 3.09 mm (range 0.73–6.07 mm, mean 3.0 ± 0.19 mm, $p < 0.05$). The smaller the stent, the less intestinal paralysis took place ($p < 0.05$): in the 18-G CASP group the lumen of the small intestine 24 h after CASP induction was 2.56 mm (range 0.97–5.38 mm, mean 2.56 ± 0.82 mm). Even the 48-h values were significantly lower than those for the 16-G CASP group where the lumen was 2.66 mm (range 1.06–8.23 mm, mean 2.66 ± 1.04 mm, $p < 0.05$) after 48 h.

Eur Surg Res 2018;59:126–142
DOI: 10.1159/000490663

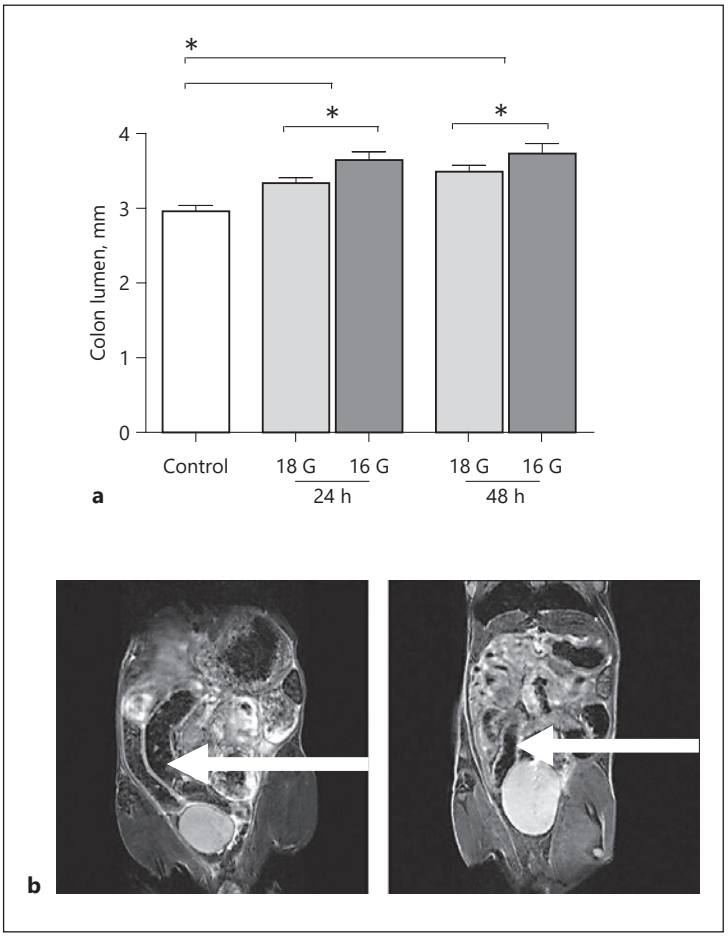

Fig. 5. a Colon lumen in control and 24 and 48 h after 18- and 16-G CASP. **b** Colon in coronal sectional images (white arrows): CASP and control. **c** Small intestine lumen in control and 24 and 48 h after 18- and 16-G CASP. **d** Small intestine in transverse sectional images (white arrows): control and CASP. **e** Stomach volume in control and 24 and 48 h after 18- and 16-G CASP. **f** Stomach in coronal sectional images (white arrows): CASP and control. Error bars indicate standard errors of the means (n = 6–10/group). * p < 0.05.

(Figure continued on next page.)

Stomach volume increased significantly in the presence of peritonitis independent of the chosen stent size (p < 0.05) (Fig. 5e, f). In the control group values of 193 mm^3 (range 167–217 mm^3, mean 193 ± 22 mm^3) for stomach volume were documented. After 24 h an average volume of 321 mm^3 was observed (range 176–451mm^3, mean 321 ± 102 mm^3). At 48 h after implantation a 16-G stent resulted in a stomach volume of 229 mm^3 (range 133–320 mm^3, mean 229 ± 131 mm^3). The detected volumes showed no differences between the use of a smaller (18-G) and larger (16-G) CASP stent: volumes after 24 h: 267mm^3 (range 181–364 mm^3, mean 276 ± 62 mm^3), volumes after 48 h: 392 mm^3 (range 164–665 mm^3, mean 392 ± 204 mm^3).

In summary, insertion of a stent into the ascending colon correlates with increased diameters of the stomach, small intestine, and colon. Interestingly, 16-G CASP caused increased lumina of the small intestines and colon, serving not only as a sign of pronounced paralysis, but also indicative of the progress of peritonitis.

Signs of Intestinal Wall Edema under Septic Conditions

Standardized monitoring of the bowel wall thickness was excellently feasible in this model. Small intestines of mice without peritonitis had a wall thickness of 0.51 mm (range 0.27–0.9 mm, mean 0.51 ± 0.15 mm). At 24 h after 16-G CASP, a wall thickness of 0.72 mm (range 0.18–1.51 mm, mean 0.72 ± 0.19 mm, p < 0.05) was determined, and 48 h after 16-G CASP a wall thickness of 0.65 mm (range 0.16–1.34 mm, mean 0.65 ± 0.16 mm, p < 0.05) was

Eur Surg Res 2018;59:126–142
DOI: 10.1159/000490663

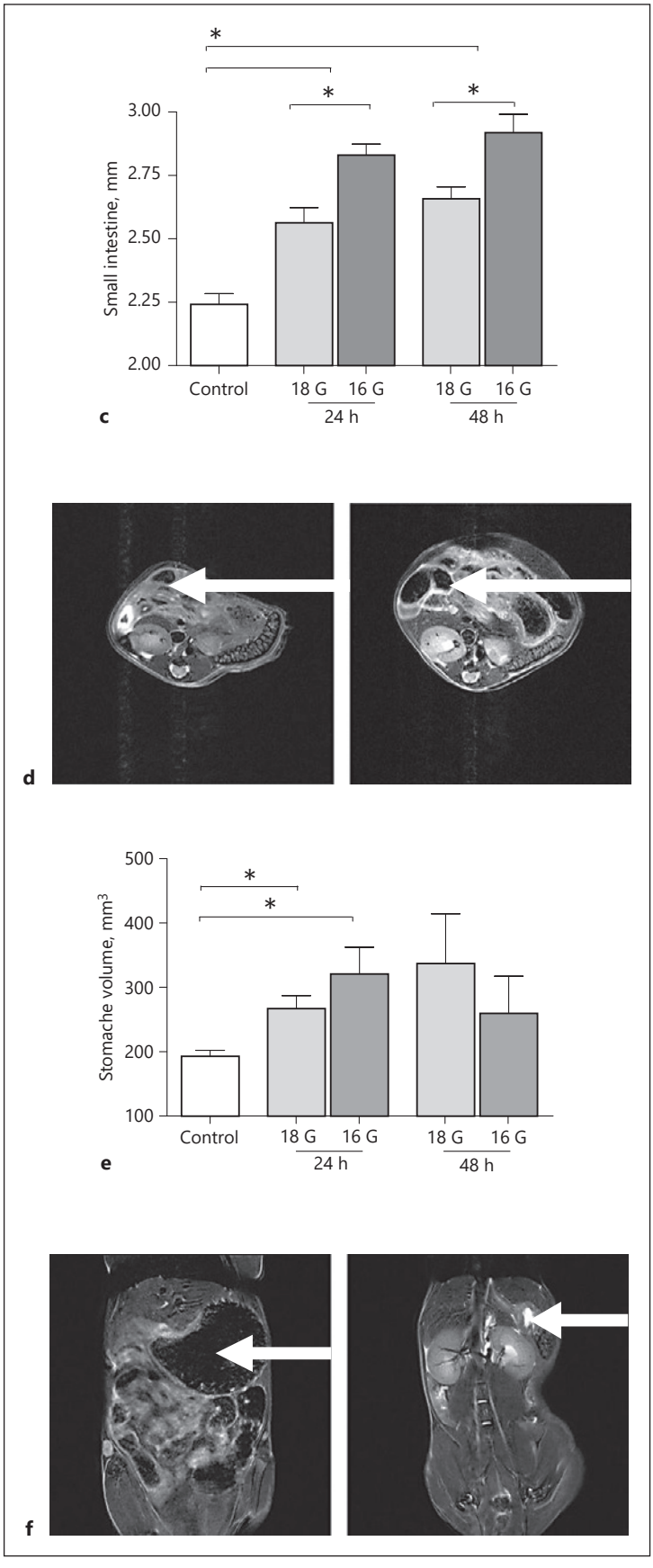

5

Eur Surg Res 2018;59:126–142
DOI: 10.1159/000490663

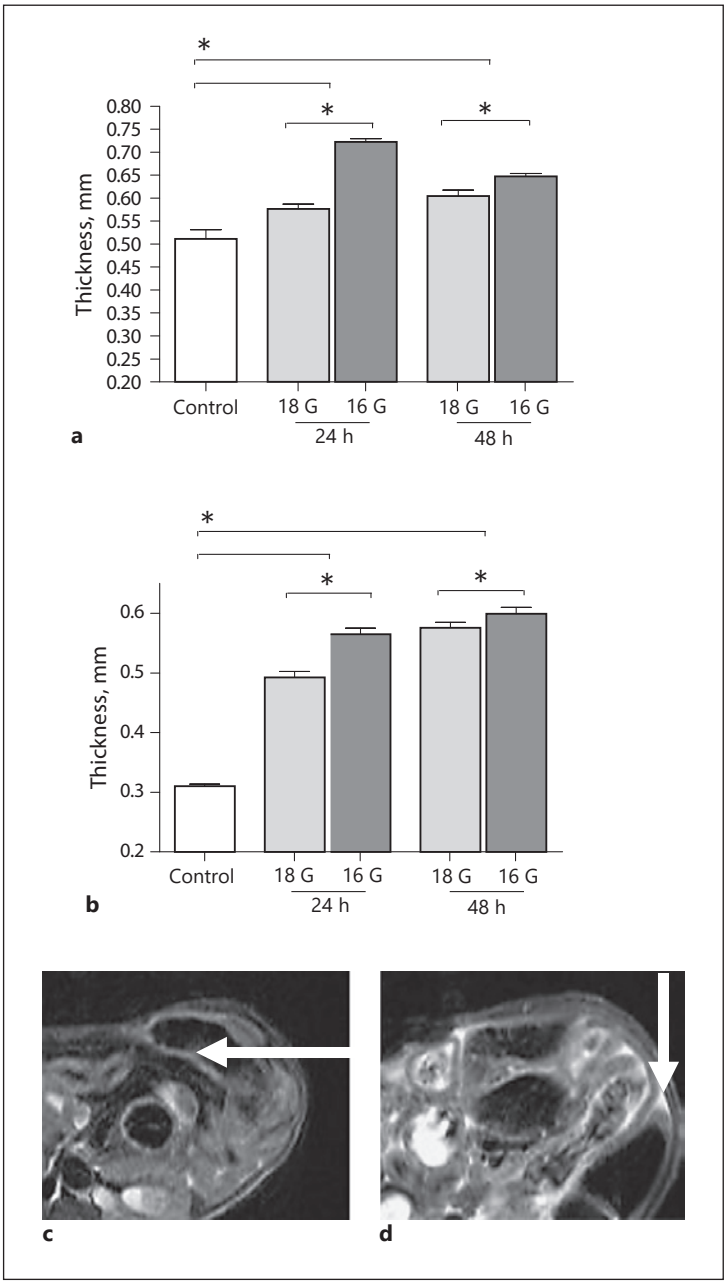

Fig. 6. a Small intestine wall thickness in control and 24 and 48 h after 18- and 16- CASP. **b** Colon wall thickness in control and 24 and 48 h after 18- and 16-CASP. Error bars indicate standard errors of the means (n = 6–10/group). * $p < 0.05$. Transverse sectional images of colon wall thickness (**c**) and free abdominal fluid (**d**) (white arrows) in CASP.

detectable. Using the smaller 18-G tube the wall of the small intestine was significantly thicker with 0.57 mm (range 0.15–1.01 mm, mean 0.57 ± 0.15 mm, $p < 0.05$) and 0.6 mm (range 0.17–1.18 mm, mean 0.6 ± 0.17 mm, $p < 0.05$) after 24 and 48 h, respectively, compared to mice without peritonitis (Fig. 6a).

Similar but less pronounced values in wall thickness were collected for the colon. The colon wall in healthy animals is much thinner than that of the small intestinal wall. Its unaffected thickness prior to CASP surgery was just 0.31 ± 0.05 mm (range 0.16–0.5 mm). In severe sepsis (16-G CASP) it was significantly higher with 0.56 ± 0.19 mm (range 0.24–1.31 mm, $p < 0.05$) after 24 h and 0.6 ± 0.15 mm (range 0.28–1.16 mm, $p < 0.05$) after 48 h. After the use of smaller stent sizes, intestinal wall edema enlargement was significantly lower ($p <$

Eur Surg Res 2018;59:126–142
DOI: 10.1159/000490663

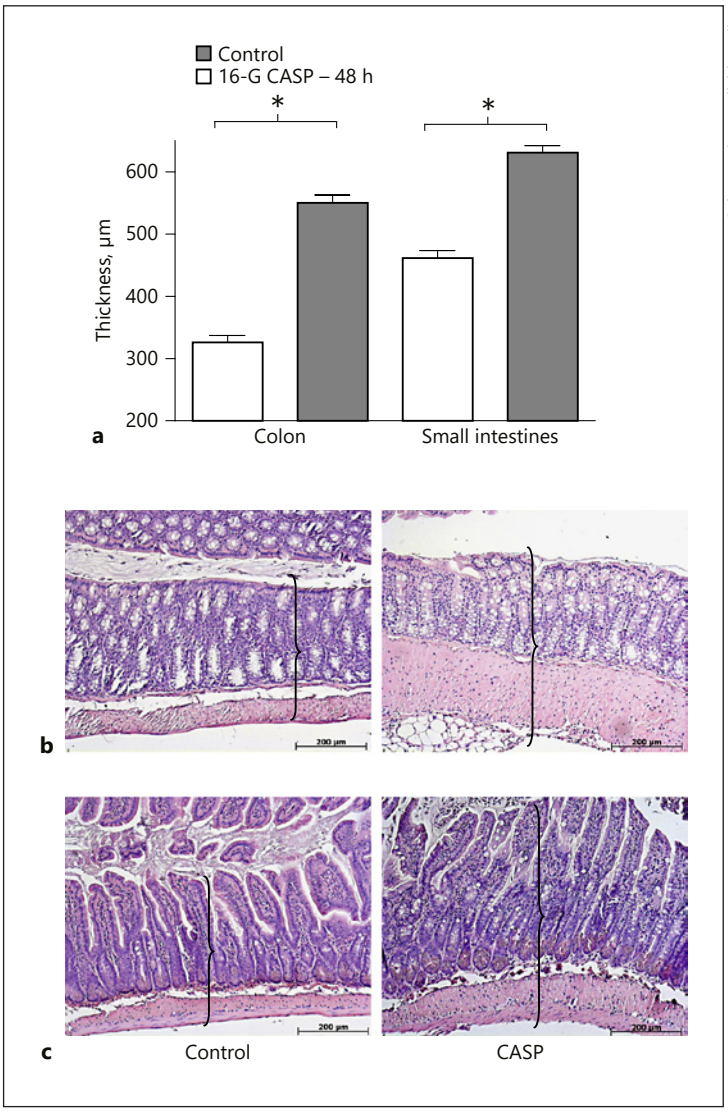

Fig. 7. a Wall thickness of colon and small intestine measured in histologic specimens in control and 48 h after 16-G CASP. Error bars indicate standard errors of the means (n = 3/group). * p < 0.001. **b** Colon: control and 48 h after 16-G CASP. HE, ×100. **c** Small intestine: control and 48 h after CASP. HE, ×100. Brackets demonstrate increased wall thickness model.

0.05). At 24 and 48 h after 18-G CASP the colon wall was 0.49 ± 0.11 mm (range 0.19–0.71 mm) and 0.57 ± 0.14 mm (range 0.24–0.97 mm), respectively (Fig. 6b).

Along with intestinal paralysis, yet another characteristic of abdominal sepsis was fluid loss in the third space. Intestinal wall edema (Fig. 6c) and free intestinal fluid (Fig. 6d) were also detected.

MRI Results Fit with Histological Findings and Macroscopic Analysis of the Situs

Histology

The unaffected small intestinal wall measured 461.6 ± 59.77 µm (range 360–550 µm). Small intestinal and colonic walls measured 326.0 ± 54.92 µm (range 270–450 µm). After CASP the small intestines measured 631.2 ± 56.15 µm (range 550–710 µm, p < 0.0001) and colon wall thickness stood at 550.40 ± 61.95 µm (range 470–680 µm, p < 0.0001) 48 h after 16-G CASP (Fig. 7a–c).

Eur Surg Res 2018;59:126–142
DOI: 10.1159/000490663

Color version available online

Fig. 8. Typical intraabdominal situs in peritonitis 48 h after 16-G CASP: distended intestines – colon (*), small intestines (#), CASP stent (black arrow).

Table 1. Parameters and score values of MRI sepsis score (MSS)

Parameter	0	1	2	3
Stomach volume, mm^3	<200	<250	<300	>350
Adrenal glands, mm^2	<1.5	1.5–1.8	2.0–2.3	>3.0
Small intestine wall, mm	<0.5	0.5–0.6	0.6–0.7	>0.7
Small intestine lumen, mm	<2.2	2.2–2.5	2.5–2.8	>2.8
Spleen volume, mm^3	<70	70–100	100–120	>120
Free fluid	–	none	stent region	diffuse

Minimum MSS: 1; maximum MSS: 18. MSS levels and interpretation: 1–5: no abdominal morphology characteristics for sepsis; 6–9: minor morphology signs for abdominal sepsis; 10–14: serious abdominal sepsis; 15–18: severe abdominal sepsis.

Macroscopy

Intraabdominal macroscopic examination substantiated the MRI findings: small amounts of free fluid were present within the abdominal cavity of septic mice. All septic animals had visible changes in morphologic abdominal findings. Increased bowel wall thickness, distended intestines, and increased volumes of spleen and stomach could be verified. The serosal surface was thickened due to bowel edema. Paralysis, edema, and vasodilatation of intestinal vessels were observed in all CASP animals as signs of generalized peritonitis (Fig. 8).

Clinical Sepsis Severity Can Be Scored by a Combination of MRI Findings

The collected MRI data of intestinal paralysis, volume shift to the third space, and alterations in organ morphology were characterized, sorted, and scored using the MSS with 1 serving as minimum and 18 as maximal score. A score of 1–5 points meant no abdominal

Eur Surg Res 2018;59:126–142
DOI: 10.1159/000490663

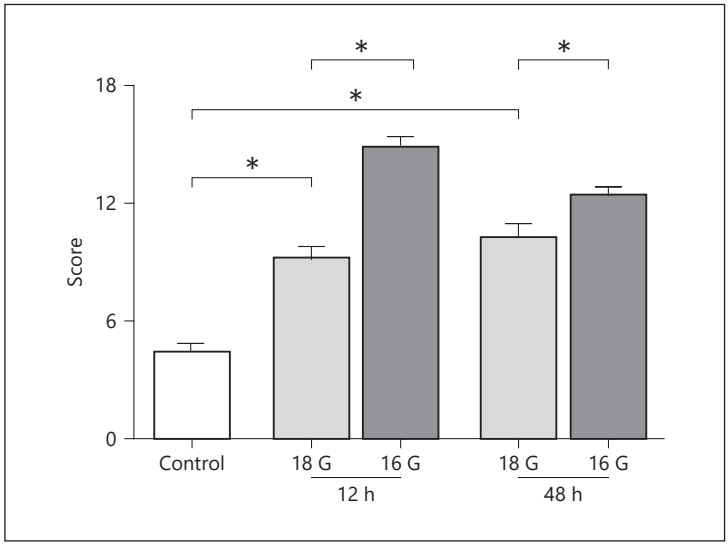

Fig. 9. MRI sepsis scores in control (timepoint 0, untreated mice) and 24 and 48 h after 18- and 16-G CASP. Error bars indicate standard errors of the means (n = 6–10/group). * $p < 0.05$.

morphology characteristics for sepsis; a score of 6–9 was classified as minor morphologic signs of abdominal sepsis; a score of 10–14 points indicated serious abdominal sepsis; and a score of 15–18 points was classified as severe abdominal sepsis (Table 1).

Control mice achieved a mean MMS score of 4.8 (range 2–6) equitable to the level of "no morphologic characteristics for peritonitis" in the MRI score system.

Augmented stent sizes led to significantly higher scores. In the case of smaller 18-G stent size after 24 h, a mean MSS of 9.2 (range 6–12, $p < 0.05$) was determined, and after 48 h the mean value stood at 10.2 (range 7–13, $p < 0.05$). At 24 h after 16-G CASP, the mean score was 14.7 (range 12–18, $p < 0.05$) and 48 h after induction of the abdominal sepsis the mean score was 12.1 (range 11–14, $p < 0.05$). The severity scores between 16- and 18-G CASP differed significantly at the two timepoints (24 and 48 h, $p < 0.05$) (Fig. 9).

Discussion

To the best or our knowledge there have been no publications reporting the impact of MRI for the monitoring of septic peritonitis in a murine model. This investigation not only describes the significant usefulness of such a tool, but also offers a simple yet innovative and easily reproducible scoring system to objectify the detected changes of peritonitis in MRI scans.

Recent MRI studies have demonstrated the innovative potential of noninvasive imaging in small animal models. Selective imaging of malignant ascites in mice is one such study [10]. Another MRI imaging model for liver regeneration could reliably and reproducibly quantify the proliferative rate of hepatocytes using MRI in rodents [11]. MRI plays an important role in the molecular and functional imaging of cancer [12]. Our group has published interesting results for noninvasive monitoring of tumor growth in a murine model for pancreatic cancer [13] and for tumor growth of pancreatic cancer following surgical trauma [14]. In inflammatory situations MRI can generate morphologic information at the site of infection by providing three-dimensional spatially resolved information. Attia et al. [15] visualized the distribution of innate immune proteins during systemic infection in mice to study inflammation during infection.

The first reports of the use of MRI in small animals were published 30 years ago [16]. Most studies investigated the development of tumor size and volume in murine tumor models.

The technique of MRI has steadily improved and has covered an increasing spectrum of applications. Nowadays, MRI technique provides a tool for clinical imaging. Due to the absence of radiation MRI is an established method to detect pathologies in children and during pregnancy. It is well accepted for the visualization of hepatobiliary disorders, diseases of the CNS, and musculoskeletal abnormalities. MRI offers high resolution in soft tissue, can be repeated without limitations, and is mostly independent from additive contrast media. It is therefore an ideal tool for examining morphologic soft tissue alterations during peritonitis.

For research applications, special small animal MRI scanners in combination with clinical devices are more and more available; 7-tesla MRI not only offers excellent imaging performance, but also provides a tool for translational research [17].

With peritonitis, typical morphologic changes such as increase in spleen volume, adrenal gland size, small bowel wall thickness and lumen, colon lumen and wall thickness, stomach volume, and intensity of free abdominal fluid were observed. MRI visualization of stomach size in polymicrobial murine sepsis has been previously described [18].

In this study, a longitudinal monitoring procedure to image changes over time was performed. The described changes of increased bowel thickening and lumen are in accordance with observations made in the abdominal cavity during peritonitis. This investigation describes the morphologic changes observed in an established murine peritonitis model (CASP model) at different timepoints in the same animal. Furthermore, the progress of peritonitis could be followed and its degree of severity classified. Comprehensive examinations led to the development of the MSS, a relatively simple but innovative score to objectify the detected changes in MRI scans. This score enables the use of the small animal MRI as a monitor for the course of a septic murine peritonitis.

The CASP model pretends to closely mimic human disease and is therefore the best compromise between standardization and clinical relevance. The usage of different stent sizes to trigger survival has already been described and is well known. Chosen stent size correlates significantly with a better or poorer survival ("standardized lethality rates") in CASP mice [7]. The 16- and 18-G CASP were used based upon the expected steadily increasing systemic inflammatory response within the groups as well as the known survival rates of 50% (18 G) and 30% (16 G), which remained basically unaffected 48 h after CASP induction [7]. Since cytokine levels do not differ significantly in various stent groups, there is no adequate conclusion for the further challenge of sepsis in the observed animal. Cytokine levels are helpful as proof of principle that mice are in a septic condition.

Until now it was merely possible to describe the lethality but not the time kinetics as well as visceral morphologic changes affected by the stent size. Therefore, MRI provides the ability to offer a new dimension to the clinical relevance of the CASP model: visualizing changes over time and visualizing differences in severity.

To demonstrate the reliability of the collected MRI data, specimens were examined histologically to compare wall thickness of the colon and small intestines in healthy mice and mice at 48 h after 16-G CASP with the detected changes in MRI. The results are very similar to one other and are comparable to observed morphologic changes in MRI under septic conditions, thereby proving the reliability of the 7-tesla small animal MRI findings.

As a further proof of principle, significant differences between MSS levels and severity of peritonitis could be detected. Increased stent sizes led to significantly higher MSS, mirroring the severity of CASP in mice.

MSS is based upon the following six pillars: free intraabdominal fluid, stomach size, wall and lumen of the intestine, spleen size, and size of adrenal glands. These six morphologies are massively involved in developing peritonitis. Parameters were not influenced due to surgical intervention itself (see online suppl. data). Therefore, measured effects can be attributed purely to CASP and sepsis.

Eur Surg Res 2018;59:126–142
DOI: 10.1159/000490663

Intraabdominal liquid and increased diameters of the intestinal organ wall as signs of fluid loss to the "third space" combined with high intraenteric volumes serve as indications of a consecutive paralytic ileus. These changes are well known and expected in patients developing abdominal sepsis [19, 20]. These observations became integrated parts of our six pillars in MSS. Lumina and wall thickness of both the colon and small intestine differed significantly depending upon "peritonitis" or "no peritonitis" status. In addition, "more peritonitis" due to a higher CASP stent size is presented by thicker walls and higher lumen of intestines as a sign of more fatal paralysis and capillary leakage.

As septic involvement of the spleen leads to higher spleen size due to a highly active immune response [21], mouse spleen size increased after the CASP procedure. Spleen volume was significantly higher according to a "more severe" peritonitis in the more lethal 16-G CASP.

The size of the adrenal gland was another predictive marker for sepsis severity in this study and was significantly higher in mice with septic peritonitis. Interestingly, the rise of adrenal gland size detected by MRI is also graduated to sepsis severity as well as seen in spleen volumes. More lethal peritonitis leads to significantly larger adrenal glands. Adrenal glands are known to have a higher volume in septic patients [22], which reflects the stress severity due to sepsis which is associated with a poor prognosis [23], and it is also known to be an independent predictor of mortality in humans [24]. The adrenocortical hypertrophy serves as evidence of increased adrenocortical function [25, 26]. As sepsis activates the hypothalamopituitary axis, corticosterone production increases very early in response to the stress of critical illness. The initial inflammatory response to sepsis activates the endogenous release of cortisol, which in turn modulates the synthesis and release of both pro- and anti-inflammatory mediators to restrict inflammation in infected tissues. Based upon this, a significant elevation of corticosterone levels was observed in septic conditions compared to control. After the peak at 12 h after CASP the values decreased significantly, which may be a sign of evolved adrenal insufficiency [23]. Adrenal gland hypertrophy could be visualized in our MRI model as an integrated part of MSS.

Taken together, standardized lethality rates represented the only readout parameter for the 18- and 16-G CASP sepsis model in the past. As a step up, MSS is a very interesting tool for evaluating new therapeutic strategies in CASP mice. New treatment approaches for diffuse peritonitis could be observed in MRI and objectified by MSS. It may perhaps provide a powerful tool for evaluation in clinical practice. A lowered MSS may reflect improvement of clinical course.

The proven, well-validated, and evaluated MSS could serve as a helpful tool for further studies in septic mice. In the timeline, repeated MRI scans could monitor treatment effects in peritonitis. MSS determined by noninvasive MRI is, in a sense, in accordance with the 3R principle (reduction, refinement, replacement), a very interesting approach in animal testing.

Conclusions

Small animal MRI enjoys the promise of great impact in the evaluation of septic peritonitis through the demonstration of early morphologic changes in the septic abdomen of mice. Repeated examinations are easy to perform using an animal as its own control. The MSS summarizes MRI-based findings reflecting macroscopic and histological alterations of the intestines. This study provides the ability to put a new dimension of clinical relevance to the CASP model: visualizing changes over time as well as differences in severity.

Acknowledgments

This study was founded by the BMBF (Bundesministerium für Bildung und Forschung Project No. 0314107, Project Name: Validierung der Magnetresonanztomographie zur Reduktion der Zahl und Belastung von Versuchstieren in der medizinischen Grundlagenforschung) and DFG-Graduiertenkolleg 840 "Host-Pathogen-Interactions."

We thank Antje Janetzko and Stefan Hadlich for excellent technical support.

Disclosure Statement

The authors declare that they have no competing financial interests.

Author Contributions

S.D., W.K., and L.I.P. designed the experiments, reviewed the data, and wrote the manuscript. J.L. and M.N. performed the surgical procedures, the MRI scans, and MRI data interpretation. A.K. and J.-P.K. performed the MRI scans. D.N.T. performed and analyzed the histology. P.M. and C.-D.H. planned the experiments and critically reviewed the manuscript before submission. All authors reviewed and approved the final version of the manuscript.

References

1 Talmor D, Greenberg D, Howell MD, Lisbon A, Novack V, Shapiro N: The costs and cost-effectiveness of an integrated sepsis treatment protocol. Crit Care Med 2008;36:1168–1174.
2 Engel C, Brunkhorst FM, Bone HG, Brunkhorst R, Gerlach H, Grond S, Gruendling M, Huhle G, Jaschinski U, John S, et al: Epidemiology of sepsis in Germany: results from a national prospective multicenter study. Intensive Care Med 2007;33:606–618.
3 Angus DC, Linde-Zwirble WT, Lidicker J, Clermont G, Carcillo J, Pinsky MR: Epidemiology of severe sepsis in the United States: analysis of incidence, outcome, and associated costs of care. Crit Care Med 2001;29:1303–1310.
4 McCullough PA, Soman SS: Contrast-induced nephropathy. Crit Care Clin 2005;21:261–280.
5 Entleutner M, Traeger T, Westerholt A, Holzmann B, Stier A, Pfeffer K, Maier S, Heidecke CD: Impact of interleukin-12, oxidative burst, and iNOS on the survival of murine fecal peritonitis. Int J Colorectal Dis 2006;21:64–70.
6 Partecke IL, Kaeding A, Sendler M, Albers N, Kuhn JP, Speerforck S, Roese S, Seubert F, Diedrich S, Kuehn S, et al: In vivo imaging of pancreatic tumours and liver metastases using 7 Tesla MRI in a murine orthotopic pancreatic cancer model and a liver metastases model. BMC Cancer 2011;11:40.
7 Maier S, Traeger T, Entleutner M, Westerholt A, Kleist B, Huser N, Holzmann B, Stier A, Pfeffer K, Heidecke CD: Cecal ligation and puncture versus colon ascendens stent peritonitis: two distinct animal models for polymicrobial sepsis. Shock 2004;21:505–511.
8 Buras JA, Holzmann B, Sitkovsky M: Animal models of sepsis: setting the stage. Nat Rev Drug Discov 2005;4:854–865.
9 Zantl N, Uebe A, Neumann B, Wagner H, Siewert JR, Holzmann B, Heidecke CD, Pfeffer K: Essential role of gamma interferon in survival of colon ascendens stent peritonitis, a novel murine model of abdominal sepsis. Infect Immun 1998;66:2300–2309.
10 Eto H, Hyodo F, Nakano K, Utsumi H: Selective imaging of malignant ascites in a mouse model of peritoneal metastasis using in vivo dynamic nuclear polarization-magnetic resonance imaging. Anal Chem 2016;88:2021–2027.
11 Wei W, Dirsch O, McLean AL, Zafarnia S, Schwier M, Dahmen U: Rodent models and imaging techniques to study liver regeneration. Eur Surg Res 2015;54:97–113.
12 Debergh I, Vanhove C, Ceelen W: Innovation in cancer imaging. Eur Surg Res 2012;48:121–130.
13 Partecke LI, Sendler M, Kaeding A, Weiss FU, Mayerle J, Dummer A, Nguyen TD, Albers N, Speerforck S, Lerch MM, et al: A syngeneic orthotopic murine model of pancreatic adenocarcinoma in the C57/BL6 mouse using the Panc02 and 6606PDA cell lines. Eur Surg Res 2011;47:98–107.
14 Menges P, Klocker C, Diedrich S, Sendler M, Maier S, Weiss FU, Heidecke CD, von Bernstorff W, Partecke LI: Surgical trauma leads to a shorter survival in a murine orthotopic pancreatic cancer model. Eur Surg Res 2015;54:87–94.

15 Attia AS, Schroeder KA, Seeley EH, Wilson KJ, Hammer ND, Colvin DC, Manier ML, Nicklay JJ, Rose KL, Gore JC, et al: Monitoring the inflammatory response to infection through the integration of MALDI IMS and MRI. Cell Host Microbe 2012;11:664–673.
16 Bottomley PA: In vivo tumor discrimination in a rat by proton nuclear magnetic resonance imaging. Cancer Res 1979;39(2 Pt 1):468–470.
17 Pinkernelle JG, Stelter L, Hamm B, Teichgraber U: Small animal MRI: clinical MRI as an interface to basic biomedical research (in German). Rofo 2008;180:505–513.
18 Kessler W, Diedrich S, Menges P, Ebker T, Nielson M, Partecke LI, Traeger T, Cziupka K, van der Linde J, Puls R, et al: The role of the vagus nerve: modulation of the inflammatory reaction in murine polymicrobial sepsis. Mediators Inflamm 2012;2012:467620.
19 Boettcher I, Gasch J, Lohr H, Lindner P: Determination of intravasal volume loss in arteria mesenterica superior shock in the rat and attempt for adequate substitution therapy (in German). Langenbecks Arch Chir 1975;(suppl):191–195.
20 Macari M, Balthazar EJ: CT of bowel wall thickening: significance and pitfalls of interpretation. AJR Am J Roentgenol 2001;176:1105–1116.
21 Taylor AJ, Dodds WJ, Erickson SJ, Stewart ET: CT of acquired abnormalities of the spleen. AJR Am J Roentgenol 1991;157:1213–1219.
22 Nougaret S, Jung B, Aufort S, Chanques G, Jaber S, Gallix B: Adrenal gland volume measurement in septic shock and control patients: a pilot study. Eur Radiol 2010;20:2348–2357.
23 Annane D: Adrenal insufficiency in sepsis. Curr Pharm Des 2008;14:1882–1886.
24 Jung B, Nougaret S, Chanques G, Mercier G, Cisse M, Aufort S, Gallix B, Annane D, Jaber S: The absence of adrenal gland enlargement during septic shock predicts mortality: a computed tomography study of 239 patients. Anesthesiology 2011;115:334–343.
25 Harvey PW, Sutcliffe C: Adrenocortical hypertrophy: establishing cause and toxicological significance. J Appl Toxicol 2010;30:617–626.
26 Akana SF, Shinsako J, Dallman MF: Relationships among adrenal weight, corticosterone, and stimulated adrenocorticotropin levels in rats. Endocrinology 1983;113:2226–2231.